VI CONGRESSO NACIONAL DE ENGENHARIA MECÂNICA
VI NATIONAL CONGRESS OF MECHANICAL ENGINEERING
18 a 21 de agosto de 2010 – Campina Grande – Paraíba - Brasil
August 18 – 21, 2010 – Campina Grande – Paraíba – Brazil

A STRUCTURAL HEALTH MONITORING SYSTEM BASED ON LAMB WAVES USING WAVELET AND FFT ANALYSIS

Vitor Ramos Franco, vrfranco86@yahoo.com.br[1]
Aldemir Aparecido Cavalini Junior, aacjunior@mecanica.ufu.br[1]
Camila Gianini Gonsalez, cggonsalez@aluno.feis.unesp.br[1]
Vicente Lopes Junior, vicente@dem.feis.unesp.br[1]

[1]GMSINT – Grupo de Materiais e Sistemas Inteligentes, Department of Mechanical Engineering, Faculdade de Engenharia de Ilha Solteira – UNESP, Av. Brasil 56, Ilha Solteira, SP, Brazil, ZIP CODE 15385000, www.dem.feis.unesp.br/gmsint

Abstract. *This paper presents an experimental technique for Structural Health Monitoring (SHM) based on Lamb waves approach in an aluminum beam using piezoelectric material as actuators and sensors. Lamb waves are a form of elastic perturbation that remains guided between two parallel free surfaces, such as the upper and lower surfaces of a plate, beam or shell. Lamb waves are formed when the actuator excites the structure's surface with a pulse after receiving a signal. Two PZTs were placed in the beam's surface and one of them was used to send a predefined wave through the structure. Thus, the other PZT (adjacent) becomes sensor and measurer of the reply signals receiving the pulses. Using this methodology, this paper presents one case of damage detection considering the aluminum beam in the free-free boundary condition. The damage was simulated by additional masses coupled on the beam's surface. The damage severity and the excitation frequency were varied, and the results were compared. For each condition, the FFT of the output signals were computed. In addition, other analysis was done, based on the wavelets analysis. The results showed the viability of the presented methodology to characterize damage in smart structures.*

Ke-words: *Structural Health Monitoring, Lamb Waves, Smart Materials, FFT Analysis, Wavelet Analysis*

1. INTRODUCTION

Nowadays, in the world of engineering, there is an interest in the development of a real-time Structural Health Monitoring (SHM) method. SHM is a system with the ability to detect and interpret adverse "changes" in a structure. An SHM system examines the structure and must provide information about any structural variation. This type of system allows systems and structures to actively monitor their own structural integrity (Inman *et al*., 2005). An SHM system typically consists of an onboard network of sensors for data acquisition and a central processor to evaluate the structural health. The development of "smart structures" has provided the necessary technology to implement in-situ monitoring systems into complex structures. With the advances in actuator technology, particularly collocated sensor-actuators, and microcomputer processing, effective and inexpensive Non-Destructive Evaluation of large complex structures can be developed. The concept of the structural integration of sensing is known as "an intelligent system" or "a smart structure". To be effective, a SHM system must provide real-time and continuous structural health assessment. The sensors must be an integral part of the structure, i.e., in-situ, in order to provide a measurement on a continuous basis (Castanien and Lian, 1996).

Considered among the most promising methods in structural dynamics for SHM, the method of interrogating a structure with high frequency waves (Lamb waves) is investigated in this paper. Many researchers have studied the technology of SHM in which piezoelectric sensors/actuators are integrated into a structure. Using these actuators and sensors it is possible to realize a structural monitoring system using Lamb waves. In particular, the use of Lamb waves can offer a way of estimating damage occurrence in a structure in terms of location, severity and type of damage. Several different applications can be cited in this area, for instance, Franco *et al.* (2009) used piezoelectric material for detecting and locating damages in plate-like structures. A set of PZT patches were attached to the plate surface for generating Lamb waves and the configuration used permitted to locate the damages with accuracy.

Perhaps the most important factor that has allowed Lamb wave techniques to flourish recently is the development of wavelet analysis. Wavelet decomposition is similar to the Fourier decomposition, however instead of just using sines and cosines, complex "mother wavelets" are used do break down the signal. The mother wavelet is essentially used as an orthogonal basis vector to filter the signal, and is scaled and shifted to approximate the frequency components of the

signal. Typically this decomposition is not done continuously since most of the mother wavelets have no closer form solutions. As result a discrete transform on buffered portions of a signal is typically used. This can be performed in commercial software packages such as MATLABTM using codes such as that presented by Kessler (2002a).

This paper presents an experimental technique of damage detection applied in a beam-like structure was used. Two PZT patches were configured as actuator and sensor, generating
and sensing Lamb waves. Structural damages were simulated by adding small masses in specific regions on the structure. The results were analyzed in two different ways: the first analysis was based on the FFT of the signals; and in the second analysis, the signals were decomposed using the Morlet wavelet. The H_2 Norm was used as index for the damage detection.

2. DESCRIPTION OF LAMB WAVES

Lamb waves are a form of elastic perturbation that remains guided between two parallel free surfaces, such as the upper and lower surfaces of a plate, beam or shell. This type of wave phenomenon was first described by Horace Lamb in 1917; however, he never attempted to produce them (Kessler *et al.*, 2002b). There are two groups of waves, symmetric (S) and anti-symmetric (A), that satisfy the wave equation and boundary conditions for this problem and each can propagate independently of the other. The symmetric group is used for damage detection in metallic structures and the anti-symmetric one is used for damage detection in composites structures. The present work utilizes PZT patches to excite the first symmetric Lamb wave mode. Lamb waves are formed when the actuator excites the structure's surface with a pulse after receiving a signal.

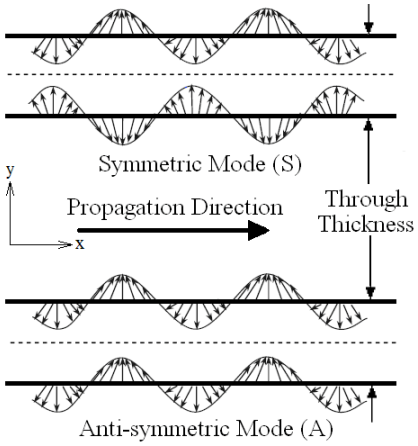

Figure 1. Graphical representation of S and A Lamb wave shapes.

The theory of Lamb waves is fully documented in a number of textbooks. Here, it's only reproduced an overview (Inman *et al.*, 2005). The analysis starts with the Helmholtz decomposition that considers the decomposition of Navier's elastodynamic vector equation

$$(\lambda + \mu)\nabla\nabla \cdot \mathrm{u} + \mu\nabla^2 \mathrm{u} = \rho\ddot{\mathrm{u}} \tag{1}$$

Letting the displacement vector **u** be expressed as

$$\mathbf{u} = \nabla\phi + \nabla \times \psi \tag{2}$$

into a scalar wave equation and a vector wave equation, given by

$$\nabla^2\phi = \frac{1}{c_L^{\,2}}\ddot{\phi}\ , \quad \nabla^2\psi = \frac{1}{c_T^{\,2}}\ddot{\psi} \tag{3}$$

where ϕ and ψ are two potential functions,

$$c_L^2 = \frac{(\lambda + 2\mu)}{\rho}, \quad c_T^2 = \frac{\mu}{\rho} \tag{4}$$

are the pressure (longitudinal) and shear (transverse) wavespeeds respectively, ρ is the mass density,

$$\mu = \frac{E}{2(1+v)}, \quad \lambda = \frac{Ev}{(1-2v)(1+v)} \tag{5}$$

are the Lamé's constants, E is the Young's modulus and v is the Poisson ratio.

Now, consider an infinite plate of thickness 2d, i.e. the domain $\Omega = \{(x, y, z) = (-\infty, \infty) \times (-\mathrm{d}, \mathrm{d}) \times (-\infty, \infty)\}$ with free surfaces (Fig. 2). Waves in the interest are in the x-y plane, and there are no variations along z, i.e. $\partial / \partial z = 0$.

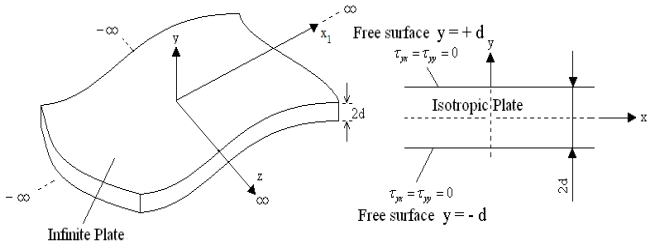

Fig. 2. Infinite plate with free surfaces

For this case, the Helmholtz's decomposition yields [1]:

$$u_x = \frac{\partial \phi}{\partial x} + \frac{\partial \psi_z}{\partial y}, \qquad u_y = \frac{\partial \phi}{\partial y} - \frac{\partial \psi_z}{\partial x}$$
$$u_z = -\frac{\partial \psi}{\partial y} + \frac{\partial \psi_y}{\partial x}, \qquad \frac{\partial \psi_x}{\partial x} + \frac{\partial \psi_y}{\partial y} = 0 \tag{6}$$

Since the boundaries y=+d and y=-d are stress free, one has:

$$\tau_{yy} = 0 \,,\ \tau_{xy} = \tau_{yx} = 0 \,,\ \tau_{yz} = \tau_{zy} = 0 \tag{7}$$

in $y = \pm d$.

To derive the equations for Lamb waves, consider first the governing equations in terms of Helmholtz scalar and vector potentials, Eq. 3. Seeking plane wave solutions in the x-y plane for waves propagating along the +x direction, assume solutions of the form:

$$\phi = (A_1 \sin py + A_2 \cos py) e^{i(\xi x - \omega t)}$$
$$\psi = (B_1 \sin qy + B_2 \cos qy) e^{i(\xi x - \omega t)} \tag{8}$$

where $\xi = \omega / c$ is the wavenumber and

$$p^2 = \frac{\omega^2}{c_L^2} - \xi^2, \quad q^2 = \frac{\omega^2}{c_T^2} - \xi^2 \tag{9}$$

The four integration constants, A_1, A_2, B_1, B_2, are found from the boundary conditions. Thus, two possible solutions result:

$$D_S = (\xi^2 - q^2)^2 \cos pd \sin qd + 4\xi^2 pq \sin pd \cos qd = 0$$
$$D_A = (\xi^2 - q^2)^2 \sin pd \cos qd + 4\xi^2 pq \cos pd \sin qd = 0 \tag{10}$$

representing the symmetric and anti-symmetric motion respectively.

Equation 10 can be rewritten in the more compact form as the Rayleigh–Lamb equation:

$$\frac{\tan qd}{\tan pd} = \left[\frac{-4pq\xi^2}{(\xi^2 - q^2)^2}\right]^{\pm 1} \tag{11}$$

where +1 corresponds to symmetric (S) motion and -1 to anti-symmetric (A) motion.

Therefore, given a certain isotropic material, Eq. 11 can be solved numerically to find the relation between the driving frequency ω and the wavenumber ξ from which the corresponding phase velocity $c_p = \omega / \xi$ can be found.

3. EXPERIMENTAL METHODOLOGY

The experimental tests were performed in an aluminum beam-like structure, in the free-free boundary condition, with two square PZTs measuring 2 cm diameter attached on its surface (Fig. 3). The beam properties and dimensions are shown in Tab.1.

Figure 3. Aluminum beam used in the experimental tests.

Table 1. Physical properties and dimensions of the plate.

Property	***Value***
Young Modulus (GPa)	*70*
Thickness (m)	*0.002*
Length (m)	*0.350*
Width (m)	*0.050*
Density (Kg/m^3)	*2710*

PZT 1 was designated as actuator, sending a predefined waveform through the structure's surface and the PZT 2 became sensor and measured the response signal. The driving pulse sent to actuate the PZT was a sinusoidal windowed with 5.5 cycles at two different drive frequencies: 15 and 20 kHz. It was used the dSPACE DS1103 Control Board for the data acquisition. Figure 4 shows the pulses sent to the PZT actuator.

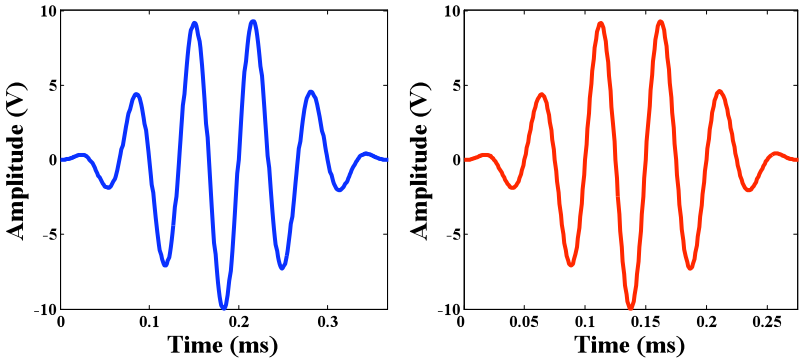

Figure 4. Sinusoidal windowed pulses sent to the PZT actuator at (a) 15 and (b) 20kHz.

The tests were realized initially in the structure without damage, getting the baseline condition. Then, another test was performed with the structure without damage, in order to compare with the baseline condition. The damages were simulated by additional masses (clamp of 1 and 3g) coupled on the structure's surface. Three sets of tests were performed, now with the addition of the damages:

- Damage Condition 1: the damage was placed in position p1 (Fig. 5);
- Damage Condition 2: the damage was placed in position p2;
- Damage Condition 3: the damage was placed in position p3.

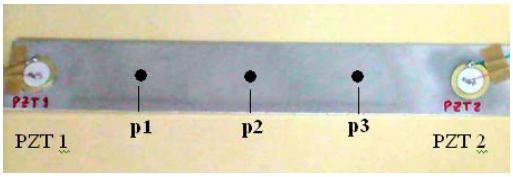

Figure 5. Position of damages on the beam's surface.

In each condition, the damage severity was changed (1 and 3g)

The signals on PZT 2 are composed for several pulses, resulting to the reflections of the actuating pulse in beam's boundaries and damages. However, only the three first pulses were considered. Figure 6 shows examples of signals obtained in the experimental tests.

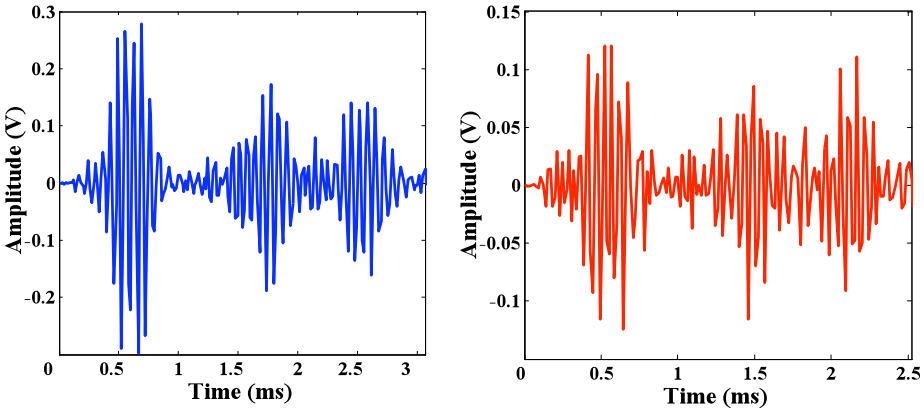

Figure 6. Examples of signals obtained in the experimental tests for (a) 15 and (b) 20kHz.

The results were analyzed in two different ways: the first analysis was based on the FFT of the signals. In the second analysis, the output signals were decomposed using the Morlet wavelet. This mother wavelet is defined as an exponentially decaying sinusoidal signal. The following equation was used for the mother wavelet (Lind, 2001):

$$\psi(t) = e^{-(1/2)t^2} \cos 5t \tag{12}$$

There are a multitude of wavelets that could be used; however, the Morlet wavelet is particularly attractive for analyzing signals that are generated by dynamical systems. Wavelet analysis relies upon a family of basis functions, called wavelets, for signal processing in the time-frequency domain (Lind, 2001).

The wavelet transform is the tool used for wavelet analysis. This transform is analogous in nature to the Fourier transform in which each process decomposes a signal into a sum of basis functions. The wavelet family is defined by the scalar parameters that represent scale and position; consequently, the wavelet transform results in a three-dimensional map. This map, *W(t)*, relates a measure of how much the signal, s(*t*), correlates with $\psi(t)$ for each value of scale and position:

$$W(t) = \int_{-\infty}^{\infty} s(t)\psi*(t)d(t) \tag{13}$$

In this analysis, a comparison between the continuous wavelet coefficients before and after the damage was performed to verify the effect of the damage in the structure. Through software MATLAB™, the continuous wavelet coefficients could be computed. The wavelet coefficient of a discrete signal *s(t)* at scale *a* and position *b* is defined by

$$C_{a,b} = \int_R s(t)\frac{1}{\sqrt{a}}\overline{\psi\left(\frac{t-b}{a}\right)}dt \tag{14}$$

where $\psi(t)$ is the Morlet wavelet.

For detecting the damage in the both analysis, the H_2 norm was used like a damage index.

The H_2 norm of a system is used to characterize the system itself, along with its modes and its sensors. Let $G(\omega)$ be a transfer function of a system. The H_2 norm of the system is defined as (Gawronski, 1998):

$$\|G\|_2^2 = \frac{1}{2\pi}\int_{-\infty}^{+\infty} \mathrm{tr}\left(G^*(\omega)(G(\omega))\right)d\omega \tag{15}$$

where tr is the trace of $G*(\omega)(G(\omega))d\omega$.

Generally, the H_2 norm is computed using modal coordinates, but in this way it is necessary to obtain a model for the equation motion. The numerical value for the H_2 norm for a SISO (single-input-single-output) system corresponds the area under the absolute value of the FFT of the system (Gawronski, 1998). In the wavelet analysis, the H_2 norm was considered like the area under the coefficients curve. In this paper, the area under of the curve was computed using the Trapezoidal method, implemented in the software Matlab® through command "trapz" (Bueno *et al.*, 2007).

The H_2 norm can be used for damage detection using the following procedure: consider the norm computed using the j*th* PZT sensor; and denoting it for a healthy structure by $\|G_{shj}\|_2$, and j*th* PZT sensor norm of a damaged structure by $\|G_{sdj}\|_2$. The j*th* sensor index of the structural damage is defined as weighted difference between the j*th* sensor norm of healthy and unknown structural conditions (damaged structure) (Gawronski and Sawicki, 2000):

$$H_{2,sj} = \frac{\left|\|G_{shj}\|_2^2 - \|G_{sdj}\|_2^2\right|}{\|G_{shj}\|_2^2} \tag{16}$$

where $H_{2,sj}$ is the H_2 Norm index, j = 1,…, r; and r is the PZT sensor number. Note that the sensor index reflects the impact of the structural damage on the j*th* sensor.

3.1. Results: FFT analysis.

Figure 7 shows the FFTs obtained to the baseline and the damage condition 1, for the mass 1g.

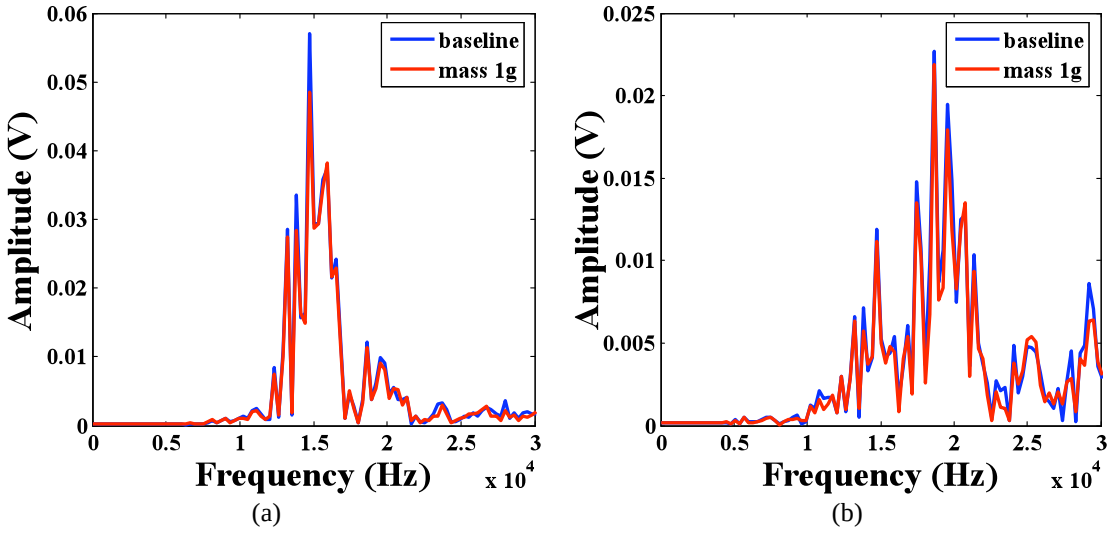

Figure 7. Examples of FFT obtained in the experimental tests at (a) 15 and (b) 20kHz.

With the FFTs obtained in all conditions, the H_2 Norm was computed. Figures 8 and 9 show the damage indexes computed using the FFT at 15 and 20 kHz respectively. In these figures, the damage position was varied.

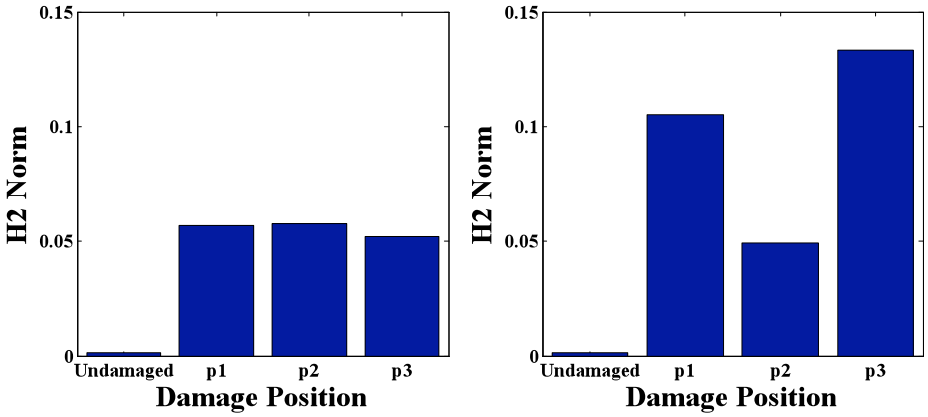

Figure 8. H2 Norm computed for FFT analysis at 15kHz: damage of (a) 1 and (d) 3g.

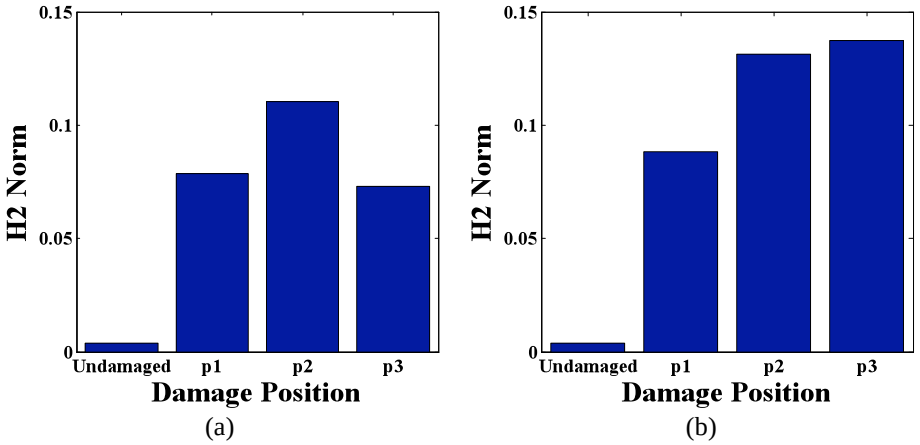

Figure 9. H2 Norm computed for FFT analysis at 20kHz: damage of (a) 1 and (d) 3g.

It's possible to observe in figure 8 and 9 the difference between the undamaged and a damage condition.

Figures 10, 11 and 12 show the indices obtained through wavelet analysis for both damages, i. e., 1 and 3g for positions p1, p2 and p3.

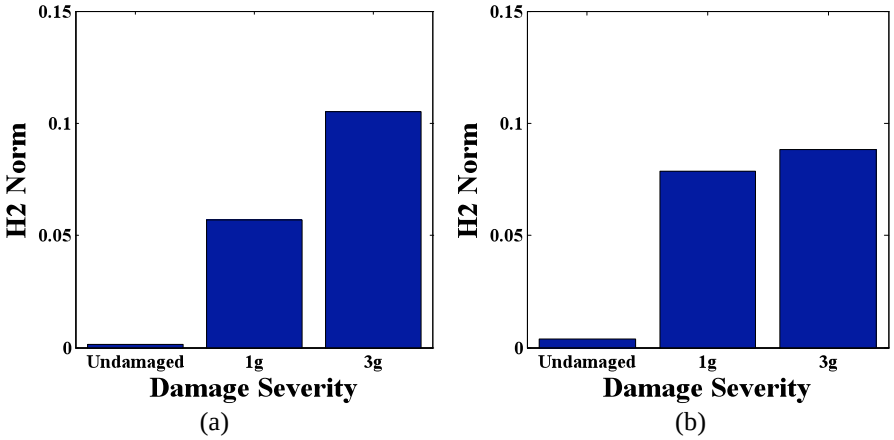

Figure 10. H2 Norm computed for wavelet analysis and damage in p1: (a) 15 and (d) 20kHz.

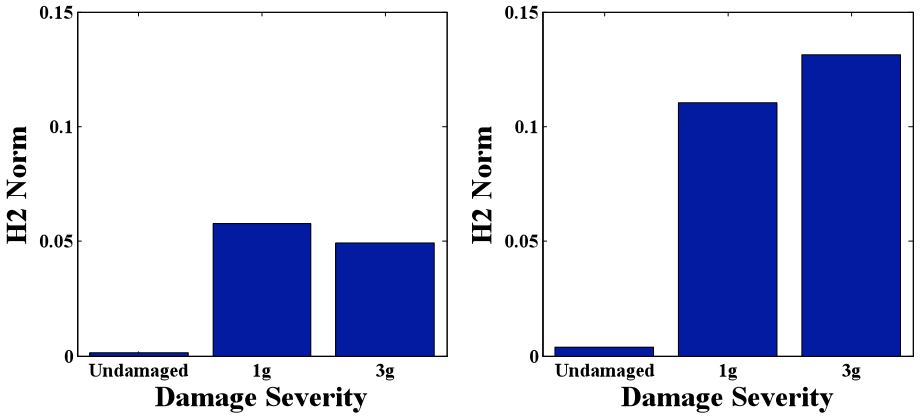

Figure 11. H2 Norm computed for wavelet analysis and damage in p2: (a) 15 and (d) 20kHz.

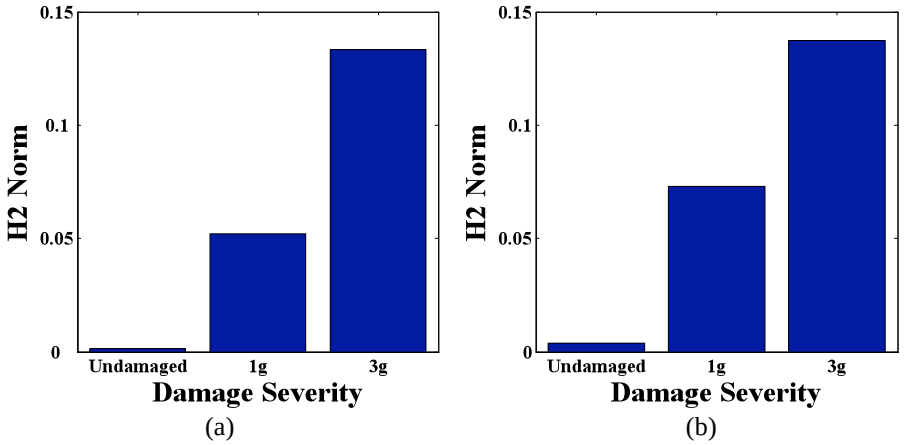

Figure 12. H2 Norm computed for wavelet analysis and damage in p3: (a) 15 and (d) 20kHz.

It's possible to observe in these figures that the indices increased when the damage severity also increased, except in Fig. 11a.

3.2. Results: wavelet analysis.

Figure 13 shows the Morlet Coefficients obtained for the baseline and for the damage in position p1 using the mass 1g.

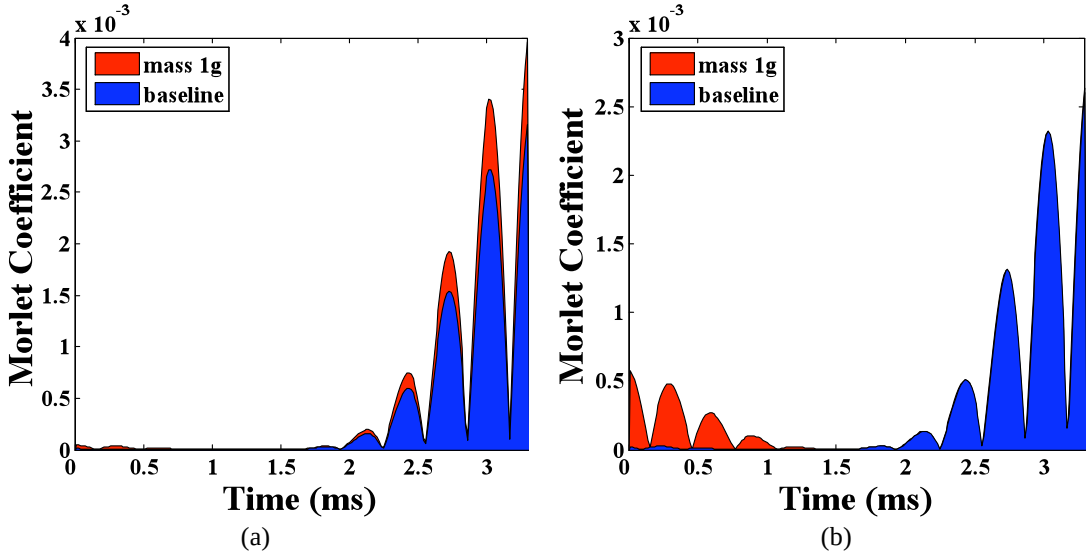

Figure 13. Morlet Coefficient curves obtained in the experimental tests for (a) 15 and (b) 20kHz.

With the Morlet Coefficient curves obtained in all conditions, the H_2 Norm was computed. Figures 14 and 15 show the damage indexes computed using the wavelet analysis at 15 and 20 kHz respectively. In these figures, the damage position was varied.

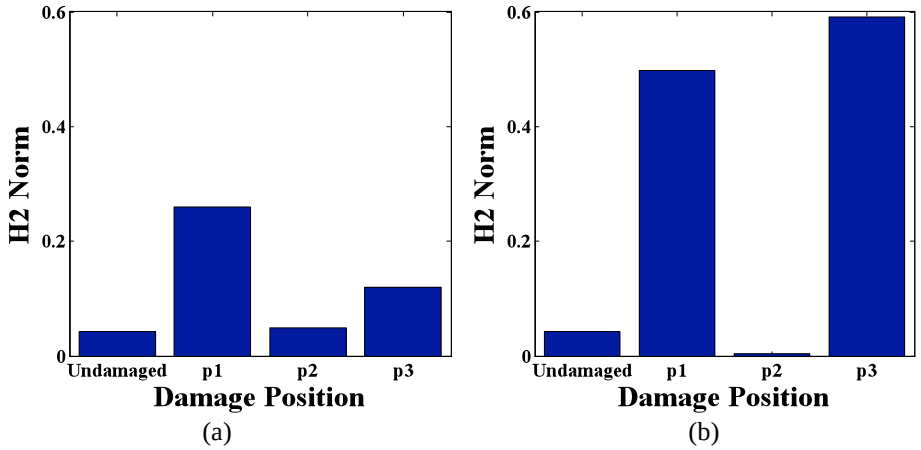

Figure 14. H2 Norm computed for wavelet analysis at 15kHz: damage of (a) 1 and (d) 3g.

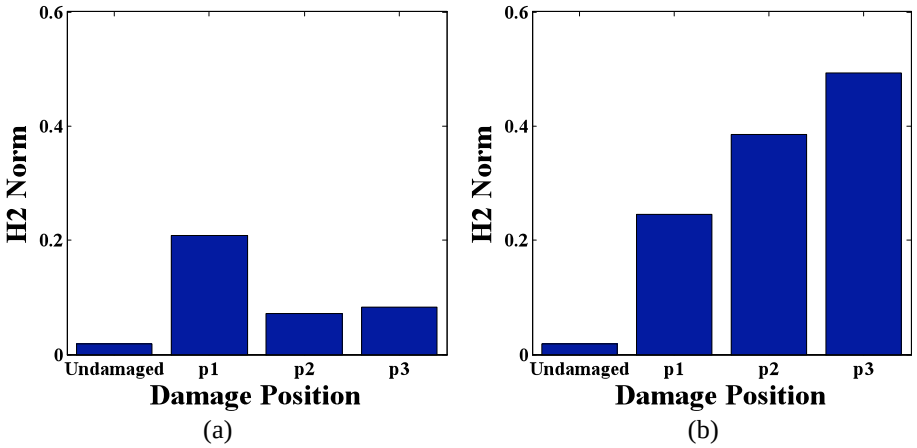

Figure 15. H2 Norm computed for wavelet analysis at 20kHz: damage of (a) 1 and (d) 3g.

It's possible to observe in figure 14 that there is a false negative for damage in position p2, i. e., the damage was not identified using this approach.

Except for damage in position p2, the indices increased when the damage severity also increased.

4. CONSLUSION AND FINAL REMARKS

In this paper a damage index involving the H_2 norm was used to detect structural damages. Lamb waves were generated using PZT patches bonded to a beam to interrogate the structure. The results were analyzed in two different ways: the first analysis was based on the FFT of the output signals. In the second analysis, the output signals were decomposed using the Morlet wavelet. In both analyses, the indices showed a difference when a damaged structure was considered, but in the second analysis, the indices were more sensitive than the FFT analysis. Further analysis must be carried out to explain the occurrence of this false negative. When the damage severity was increased, the indices also increased, except in Damage Condition 2, for damage of 3g at 15kHz. By comparing the results for different frequencies, the results obtained to 20kHz were better than the results at 15 kHz, since the indices got increased when the damage is closer to the PZT sensor, what is expected. In general, the damage detection technique presented in this paper was capable of to interrogate the structure using Lamb waves methodology applied with the use of piezoelectric patches.

5. ACKNOWLEDGEMENTS

The authors are thankful to CNPq and FAPEMIG for partially funding the present research work through the INCT-EIE and to the members of GMSINT – Group of Smart Materials and Systems.

6. REFERENCES

Bueno, D.D., Silva, S., Marqui, C.R. and Lopes Jr., V.,2007, "Compartive Study of Damage-Sensitive Indices Used for Structural Health Monitoring of Smart Structures", in 19th International Congress of Mechanical Engineering - COBEM, Brasília, DF.

Castanien, K. E. and Lian, C.,1996, "Application of active structural health monitoring technique to aircraft fuselage structures", SPIE: Smart Structures and Materials 1996, Vol 2721, pp. 38-49.

Franco, V. R., Bueno, Brennan, M.J., Cavalini Jr., Gonsalez, C.G. and Lopes Jr, V., 2009, "Experimental Damage Location in Smart Structures Using Lamb Waves Approaches", in 8th Brazilian Conference on Dynamics, Control and their Applications – DINCON 2009, Bauru, SP, Brazil.

Gawronski, W. K. and Sawicki, J.T., 2000, "Structural Damage Detection Using Modal Norms", Journal of Sound and Vibration, pp 194-198.

Gawronski, W.,1998, "Dynamics and Control of Structures, A Modal Approach", 1. Ed. New York, Springer Verlag.

Inman, D. J., Farrar, C. R., Lopes Jr., V. and Steffen Jr, V.,2005, "Damage Prognosis for Aerospace, Civil and Mechanical Systems." 01. ed. West Sussex: John Wiley & Sons Ltda, v. 01. 449 p.

Kessler, S.S., 2002a, "Piezoelectric-based in-situ damage detection of composite materials for structural health monitoring systems", Thesis (Doctorate), Massachusetts Institute of Technology, Cambridge.

Kessler, S. S., Spearing, S. M. and Soutis, C., 2002b, "Damage detection in composite materials using Lamb wave methods" Smart Materials And Structures, 11, pp. 269–278.

Lopes Jr., V., Park, G., Cudney, H. H. and Inman, D. J., 2000, "Impedance based structural health monitoring with artificial neural networking". *Journal of Intelligent Material Systems and Structures*, v. 11, p. 206-214.

Park, G., Cudney, H. and Inman, D. J.,2000, "Impedance-based Health Monitoring of Civil Structural Components", ASCE/Journal of Infrastructure Systems, v. 6, n. 4, p. 153-160.

Rytter, A.,1993, Vibration based inspection of civil engineering structures. Ph.D. Dissertation, Department of Building Technology and Structural Engineering, Aalborg University, Denmark.

7. RESPONSIBILITY NOTICE

The authors are the only responsible for the printed material included in this paper.